

DISK–JET CONNECTION IN THE MICROQUASAR GRS 1915+105 AND IR AND RADIO EMISSION

J. S. YADAV¹

Tata Institute of Fundamental Research, Homi Bhabha Road, Mumbai 400 005, India

Accepted for publication in ApJ (Part 1)

ABSTRACT

We present evidence of a direct accretion disk – jet connection in the Galactic microquasar GRS 1915+105 based on our analysis of RXTE/PCA data with a “spike” in X-ray light curves. We find that the radio emission increases as the hardness ratio increases during the low hard state. We suggest that the “spike” which separates the dips with hard and soft spectra marks the beginning of the burst phase when the luminosity of the soft X-rays (5–15 keV) increases by a large factor (~ 10). This produces a major ejection episode of the synchrotron - emitting plasma termed as “baby jets” which are associated with infrared (IR) and radio flares of about half an hour period widely reported in the literature. Subsequent short but frequent soft dips produce overlapping faint flares which result in an enhanced level of quasi-steady emission. We discuss the differences between “baby jets” and relativistic radio jets and especially investigate their signatures in X-rays.

Subject headings: accretion, accretion disks — binaries: close — black hole physics — stars: individual (GRS 1915+105) — X-rays: stars

1. INTRODUCTION

Two Galactic X-ray transient sources GRS 1915+105 and GRO J1655-40 are known to produce relativistic radio jets (Mirabel & Rodriguez 1994; Tingay et al. 1995). The combination of relativistic jets and a suspected central black hole has earned these two objects the name “microquasars” as they seem to be stellar mass analogs of the massive black hole systems in quasars and other active galactic nuclei (AGNs) (Morgan et al. 1997; Belloni et al. 1997b; Orosz & Bailyn 1997). Since microquasars are much smaller, closer and show faster variability than the extragalactic systems, they are potential “laboratories” for the study of black hole accretion/relativistic jet systems. GRS 1915+105 has shown spectacular X-ray variability since its discovery in 1992 (Castro-Tirado et al. 1994). Recently, Belloni et al. (2000) have classified a large sample of RXTE/PCA observations in 12 separate classes on the basis of their light curves and the color-color diagrams. Out of these, the β class is described as the most complex, has all the three basic states of the source (Belloni et

al. 2000), and is always accompanied by IR/radio flares. The presence of a “spike” in the X-ray light curve, which separates the dips with hard and soft spectra, clearly distinguishes this class from others. The “spike” coincides with the beginning of IR flares seen during simultaneous X-ray and IR observations, suggesting its role in initiating IR flares (Eikenberry et al. 1998). These flares are termed as “baby jets” from energy consideration. Another simultaneous observations of GRS 1915+105 in the X-ray, IR, and radio wavelengths confirm that the IR and radio flares are associated with the X-ray dips (Mirabel et al. 1998).

At present, the disk-jet connection is indirect at best for relativistic radio jets. Harmon et al. (1997) have shown a long-term correlation between hard X-ray flux and jet activity in GRS 1915+105. Fender et al. (1999) have observed four relativistic radio ejections in 1997 October/November and have presented high quality MERLIN radio images of ejecta in 400–5000 AU scales which are consistent with ballistic motion. Recently, Eikenberry et al. (2000) have reported detection of faint IR flares and have clas-

¹jsyadav@tifr.res.in

TABLE 1
SUMMARY OF THE SELECTED OBSERVATIONS OF GRS 1915+105

Observation ID	Date	Exposure (s)	PCU ^a on	Radio ^b Flux (mJy)	Infrared (IR) or Radio flares Period (min)	Peak ampl.(mJy)
10408-01-38-00	1996 Oct 07	7000	5	3	-	-
20186-03-03-01	1997 Aug 14	10000	5	29	~ 30	~ 12 [†]
20402-01-45-03	1997 Sep 09	10000	4	47	~ 30	~ 60 [§]
20402-01-52-01	1997 Oct 30	4000	5	200	~ 25	~ 200 [‡]
20402-01-53-00	1997 Oct 31	10000	5 ^c	170	~ 30	~ 150 [‡]

[†] IR flares (2.2 μ m) Eikenberry et al. 1998, [§] Radio flares (8.3 GHz) Mirabel et al. 1998, [‡] Radio flares (15 GHz) Fender et al. 1999.

^aNumber of Proportional Counter Units (PCUs) operating at the time of observation.

^bRadio flux is obtained by interpolation of 8.3 GHz public domain data from NSF-NRAO NASA except on 1996 Oct. 7 for which data are for 15.2 GHz estimated from figure 4 of Pooley & Fender (1997).

^cExcept in the time range of 1.20887×10^8 to 1.20889×10^8 (MJD ~ 50752.6) when only 3 PCUs were on.

sified the ejection events associated with IR and radio flares into three classes: (A) the relativistic events producing bright superluminal radio jets of ~ 1 Jy with decay times of several days (Mirabel & Rodriguez 1994 ; Fender et al. 1999), (B) the “baby jets” associated with ~ 100 – 200 mJy IR and radio flares with decay times of several minutes (Eikenberry et al. 1998; Mirabel et al. 1998), and (C) faint IR flares with peak amplitude of ~ 0.5 mJy and duration of 8–10 minutes (Eikenberry et al. 2000). In this paper we present the results of our detailed analysis of RXTE/PCA observations spread over a year of β and λ classes which actually belong to the same class as shown here. We investigate the role of the “spike” in initiating the “baby jets” and study the accretion disk corresponding to IR/radio flares of varying peak amplitudes (Table 1). We present evidence of a direct disk – jet connection for radio ejections of class A. We discuss the dissipation of accretion energy in the inner part of the disk in terms of a comptonising cloud and the escaping mass which produces synchrotron radiation.

2. OBSERVATIONS AND ANALYSIS

The observations discussed here are selected from the publicly available RXTE/PCA data for the X-ray transient source GRS 1915+105 (Jahoda et al. 1996). In Table 1 we list de-

tails of these observations. The source was in a high/flaring state during these observations. A portion of 2–13 keV light curves for different days added for all available PCA units are shown in Figure 1. The “spike” is present in all the observations shown in Figure 1 (all of them belong to class β) and IR/Radio flares were observed during these observations. The peak amplitude of IR/radio flares are given in Table 1. The IR flares with a spacing of ~ 30 minutes were observed during simultaneous X-ray/IR observation on 1997 August 14 (Eikenberry et al. 1998). During another simultaneous observation in the X-ray, IR, and radio on 1997 September 9, similar flares were seen in both the IR and radio bands (Mirabel et al. 1998). Fender et al. (1999) have observed four relativistic radio jets during 1997 October/November and have seen radio flares on 1997 October 30-31 in 15 GHz band (see their figure 7). The other observation of 1996 October 7 belongs to class λ (shown in Figure 2) which is a “radio-quiet” state. Munro et al. (1999) have defined the “radio-quiet” state when the radio flux in the 8.3 GHz band (or the 15 GHz band) is less than 15 mJy. The general approach of our analysis is described elsewhere (Yadav & Rao 2000). The two X-ray colors HR_1 and HR_2 are defined as the ratio of the flux in the 5–13 keV band to flux in the 2–5 keV band and the ratio of the flux

in the 13–60 keV band to flux in the 2–13 keV band respectively. The sub-second rms variability is calculated from 0.1 s data.

To study the spectral properties during these observations, we have used simultaneous fits to the PCA data in the energy range of 5–60 keV and the HEXTE data in the energy range of 15–100 keV. We used “Standard 2” mode PCA data (16 s time resolution) with 128 channel spectra and 1% systematic error added. The 64 channel archive mode data of HEXTE (cluster 0) was rebinned to improve the statistics of the counts. We have used a sum of a multicolor disk black body (DISKBB) and a power law to approximate the energy spectrum (Yadav 2000).

3. RESULTS AND INTERPRETATION

The light curves seen on 1997 October 31 (class β) and on 1996 October 7 (class λ) are shown in the top panels of Figure 2. The HR_2 color is shown in the middle panels and sub-second mean variability is shown in the bottom panels of Figure 2. In the top panels, durations of the low hard state (quiescent phase), the high soft state (burst phase) and the soft dips (low soft state) are marked by ‘C’, ‘B’ and ‘A’, respectively. Although Belloni et al. (2000) have found short soft dips of state ‘A’ in the class λ (in the beginning of burst phase and during the fast fluctuations), we have marked it whole as state ‘B’. This is done to emphasize the long dips of state ‘A’ found in class β . The HR_2 is high (0.09–0.12) during the quiescent phase (state C) whereas it is low (0.03–0.06) during the burst phase (state B) and the soft dips (state A). The similarity of the two plots in the middle panels suggests that the “spike” in the light curves of class β marks the beginning of the burst phase. This is shown by a vertical arrow in the top left panel. The mean variability plotted in bottom panels is consistent with this suggestion. The mean variability is 2–5 % during the burst phase, 10–15 % during the quiescent phase and 5–9 % during the soft dips. In the region of fast fluctuations during phase B of both the classes, the mean variability is mostly in the range of 5–9% indicating the presence of short soft dips during these fast oscillations. These results suggest that classes λ and β of Belloni et al. (2000) are very similar except for (1) the presence of long soft dip in the beginning of the burst phase in case of class β while it is short and shallow in case of class λ (see figure 4 of Belloni et al.

(2000)), and (2) the short but frequent soft dips during the fast oscillations are relatively deeper and for longer times in case of class β than that in class λ . It may be noted here that the HR_2 distinguishes the quiescent phase from other two phases (the burst phase and the soft dips) while the mean variability highlights the difference between the burst phase and the soft dips.

The class β has been studied simultaneously in IR and radio bands. Eikenberry et al. (1998) have compared X-ray and IR profiles during 1997 August 14 observations and have found that the spikes in the X-ray band coincide with the beginning of IR flares (see their figure 3). The IR intensity reaches its peak flux shortly after the X-ray peak. The IR flares have decaying phases very similar in their smoothness and time scale to the rising phases. On the other hand, the X-ray flux begins the fast oscillations after reaching their peak level as mentioned earlier. An excess in IR is seen during the fast X-ray oscillations. This excess in IR is explained in terms of many faint IR flares superposed on one another (Eikenberry et al. 2000). If we assume that each X-ray oscillation has an associated faint IR flare, an IR excess of 1.3 mJy is estimated, which is consistent with the observed excess of ~ 1.0 mJy for 1997 August 14 observations. During another simultaneous observation of β class in IR and radio on 1997 September 9, Mirabel et al. (1998) confirmed the role of the spike in initiating IR flares and have found that the radio flares follow the IR flares with a time delay consistent with broad band synchrotron emission. The profiles of IR and radio flares are quite similar. In contrast, the λ class belongs to radio-quiet state. Pooley & Fender (1997) have observed GRS 1915+105 in radio during 1996 October but no radio flares were reported during observations of λ class X-ray activity on 1996 October 7.

To investigate further the similarities and differences between β and λ classes, we have studied the mean X-ray color HR_1 , which is a measure of soft photons and hence the disk temperature. On the other hand, HR_2 is a measure of hard photons and a indicator of appearance/disappearance of the advective/halo disk (Yadav et al. 1999). The mean HR_1 during the quiescent phase is plotted as a function of mean quiescent flux in Figure 3 for all the observations in Table 1. The mean HR_1 increases with the quiescent flux and follows a single path. The HR_2 during the quiescent phase also

TABLE 2
SIMULTANEOUS SPECTRAL FITS TO PCA AND HEXTE DATA IN THE ENERGY RANGE 5–100 keV

Date	Quiescent phase (hard dips)(C)	Soft dip (A)	Burst phase (B)	Luminosity ratio (5–15 keV)	Luminosity ratio (20–100 keV)
1996 Oct 07	$T_{in} = 1.11 \pm 0.03$ $\Gamma = 2.23 \pm 0.03$ $\chi^2_{\nu} = 0.75$ $R_{in} = 37.9$ $\dot{m} = 2.19 \times 10^{18}$		$T_{in} = 2.23 \pm 0.01$ $\Gamma = 3.59 \pm 0.04$ $\chi^2_{\nu} = 1.10$ $R_{in} = 25.2$ $\dot{m} = 1.08 \times 10^{19}$	$B/C = 10.16$	$B/C = 0.52$
1997 Oct 30	$T_{in} = 0.87 \pm 0.26$ $\Gamma = 2.78 \pm 0.02$ $\chi^2_{\nu} = 1.40$ $R_{in} = 44.7$ $\dot{m} = 1.40 \times 10^{18}$	$T_{in} = 2.01 \pm 0.04$ $\Gamma = 3.77 \pm 0.04$ $\chi^2_{\nu} = 0.83$ $R_{in} = 16.2$ $\dot{m} = 1.89 \times 10^{18}$	$T_{in} = 2.13 \pm 0.02$ $\Gamma = 3.57 \pm 0.04$ $\chi^2_{\nu} = 0.80$ $R_{in} = 23.2$ $\dot{m} = 6.94 \times 10^{18}$	$B/C = 3.01$ $A/C = 1.46$ $B/A = 2.06$	$B/C = 0.43$ $A/C = 0.20$ $B/A = 2.17$

T_{in} is the temperature of the inner accretion disk in keV, Γ is the power law index, R_{in} is the characteristic radius of the inner accretion disk in km with error of $\leq 10\%$ and \dot{m} is the accretion rate in g s^{-1} .

shows similar results except it decreases with the quiescent flux (in the inset of Figure 3). These results reinforce the above suggestion that classes β and λ are very similar and actually belong to a single class.

We have studied the spectral properties of both β and λ classes using simultaneous fits to PCA and HEXTE data in the energy range 5–100 keV as described in the previous section. The segments of the quiescent phase, the burst phase, and the soft dips are analysed separately. We have selected β class data of 1997 October 30 (Figure 1c) for spectral analysis as the first relativistic jet observed by Fender et al. (1999) was close to this X-ray observation, and also the λ class data of 1996 October 7 (Figure 2 right panels). The characteristic radius of the inner disk, R_{in} is derived from the best-fit spectral parameters and the known distance and inclination (the latter is taken as the same as the inclination of the radio jets to the line of sight). From R_{in} and T_{in} , we infer the mass accretion rate using $\dot{m} = 8\pi R_{in}^3 \sigma T_{in}^4 / 3GM$ where σ is Boltzmann constant, G is the gravitational constant and M is the mass of the black hole. The value of R_{in} , which is smaller during the burst phase, cannot be less than the innermost stable orbit around a black hole. For a Schwarzschild black hole ($R_{in} \geq 6GM/c^2$), an R_{in} of ~ 20 km during the burst phase puts $M \lesssim 2.4 M_{\odot}$ (Belloni

et al. 1997a). The best-fit parameters are given in Table 2. Note that the derived values for the inner disk radius can be an underestimate due to scattering effects and the approximations made in fitting the Comptonised part of the spectrum as a power-law (see Shrader & Titarchuk 1998). We use these numbers here only for a qualitative description.

The results in Table 2 are consistent with the general picture: the spectrum is hard during the quiescent phase ($\Gamma \sim 2.5$) and it is soft during the burst phase ($\Gamma \sim 3.6$). The soft X-ray luminosity (5–15 keV) increases over a factor of ten during the burst phase while the hard X-ray luminosity (20–100 keV) reduced to half than that during the quiescent phase for 1996 October 7 observations. The total X-ray luminosity (5–100 keV) drops by a factor of ~ 5.5 during the quiescent phase than that in the burst phase. Yadav et al. (1999) have suggested that the change of states during the flaring of the source (like during class λ) is due to the appearance/disappearance of an advective/halo disk. If we assume the above scenario, most of the energy ($\sim 80\%$) disappears during the quiescent phase through advection into black hole (Narayan et al. 1997). During the quiescent phase, the total X-ray flux in the 5–100 keV band is increased from a value of 7.1×10^{-9} $\text{erg s}^{-1} \text{ cm}^{-2}$ on 1996 October 7 to a value of 16.4

$\times 10^{-9}$ erg s $^{-1}$ cm $^{-2}$ on 1997 October 30 while the B/C ratio for 5–15 keV X-ray is reduced from 10.16 to a value of 3.01 (see Table 2). The simplest explanation of these results may be that the disk disrupts due to mass ejection on 1997 October 30 before X-ray luminosity could reach its peak value during the burst phase. During the burst phase the 5–100 keV X-ray flux is $\sim 3.4 \times 10^{-8}$ erg s $^{-1}$ cm $^{-2}$ on 1997 October 30 whereas it is $\sim 3.9 \times 10^{-8}$ erg s $^{-1}$ cm $^{-2}$ on 1996 October 7 when short, soft dips were observed by Belloni et al. (2000) as discussed earlier which suggest the beginning of mass ejection (radio flux is still low, see Table 1). These results indicate a luminosity threshold to start the disk evacuation which produces the long, soft dip after a spike in the X-ray light curve.

The B/A luminosity ratio is ~ 2 in the whole range of 5–100 keV on 1997 October 30 (see Table 2) while Γ increases to 3.77 during the soft dip from a value of 3.57 during the burst phase suggesting a portion of the inner disk and the halo are blown away/disappears during the soft dips. Feroci et al. (1999) have also proposed of a disappearance of the inner disk during soft dips from BeppoSAX observations of GRS 1915+105. Note that the viscous time scales of the inner disk and that of the halo have almost same value of about 1 s which agrees with the fall time scale of the soft dips (Belloni et al. 2000; Yadav et al. 1999). As the halo disappears more disk is observable reducing the R_{in} during the soft dips (see Table 2). Note here that the “spike” marks the beginning of the burst phase as described earlier. The accretion rate is reduced from $\sim 6.94 \times 10^{18}$ g s $^{-1}$ during the burst phase to $\sim 1.89 \times 10^{18}$ g s $^{-1}$ during the soft dip phase suggesting $\sim 5 \times 10^{18}$ g s $^{-1}$ mass is being blown away during these soft dips. In the above scenario, the missing energy of X-rays in the 5–100 keV range during the major soft dips is $\sim 1.4 \times 10^{39}$ erg s $^{-1}$ using the known distance of the source. Fender et al. (1999) have estimated a minimum power of $\sim 2 \times 10^{39}$ erg s $^{-1}$ is required for 12 hours of rising time of the relativistic radio jets observed on 1997 October/November on the basis of equipartition of energy. Including one proton for each electron approximately doubles this energy and requires a mass flow rate of $\geq 10^{18}$ g s $^{-1}$. The energy requirement is broadly in agreement with our estimate of missing X-ray energy (5–100 keV) of $\sim 1.4 \times 10^{39}$ erg s $^{-1}$ as X-rays below 5 keV should

significantly increase this estimate. During the soft dip, the accretion rate drops by $\sim 5 \times 10^{18}$ g s $^{-1}$ from that during the burst phase which is in agreement with the required mass outflow rate.

The average radio flux is given in Table 1 for all X-ray observations discussed here. As HR_1 increases the radio flux also increases. The peak amplitude of IR/radio flares also increases with HR_1 during class β observations (Table 1). Our spectral analysis has suggested that X-ray luminosity increases with HR_1 . In Figure 4 we show the radio flux at 2.25 GHz from the NSF-NRAO-NASA Green Bank Interferometer for 1997 October 30-31 (data for ~ 48 hours) on the y-axis (left). The X-ray average color HR_1 during the quiescent phase is plotted on the y-axis (right) during the same time (data for ~ 24 hours). The timing of our X-ray data falls between the first and second relativistic radio jets observed by Fender et al. (1999). Clearly, results shown in Figure 4 suggest a correlation between the radio and X-ray data. A least-square fit to the HR_1 and radio data results a relation $radio_{Jy} = 0.615 \times HR_1 - 0.322$ with correlation coefficient close to one. This linear relation is based on a limited set of data and is valid in a narrow range of HR_1 from 0.94 to 1.2 during the relativistic radio jets. The issues like extrapolation of this relation beyond the valid range of HR_1 , its applicability during the baby jets and fitting a non-linear relation (instead of a linear relation) will be discussed separately (Yadav 2000). In Figure 5, we show the decay profile of this radio flare observed during 1997 October 30 - November 6 (offset by 50748.2 MJD). The profile is consistent with an exponential decay having a time constant of 3.157 day (dotted line). We have also plotted the decay profile of another radio flare of class A observed on 1999 June 8-15 (offset by 51334.5 MJD) in Figure 5. This flare has been observed in the X-ray band by IXAE/PPC (Naik et al. 2000) as well as partially by RXTE/PCA. The decay profiles of these two flares of class A (\sim two years apart) are identical except some deviation in the middle (on days 6 through 8). The average X-ray color HR_1 during the low hard state is also plotted in Figure 5 for both the radio flares using the linear relation between the HR_1 and radio flux density described above. These points are in good agreement with the decay profiles over the duration of observations when the radio flux drops by a factor of ~ 2 .

Let us summarise the physical picture emerging here. When the source changes state from a quiescent phase to the burst phase, the soft X-ray luminosity increases by a large factor (~ 10). If the total X-ray luminosity is above a certain threshold, it promptly triggers a major ejection event of synchrotron - emitting plasma producing a large soft dip after a spike in the X-ray light curve. Subsequent short but frequent dips and the undetectable continuous ejection during the burst phase, and probably also during the quiescent phase (if HR_1 is high), produce an enhanced level of quasi - steady emission. This conclusion agrees with the observations of faint IR flares during the hard state which start even before the X-ray oscillations (Eikenberry et al. 2000). On 1997 October 30, the total 5–100 keV X-ray flux during the quiescent phase was similar to that found during a “plateau” state ($\sim 1.7 \times 10^{-8}$ erg s $^{-1}$ cm $^{-2}$) with the enhanced quasi-steady radio emission of ~ 50 mJy (15 GHz) lasting for 20 days (Fender et al. 1999) which would suggest mass ejection during the quiescent phase. It is also consistent with the value of $k = 2$ (suggesting continuous jets) derived from the flux densities of approaching and receding components of the relativistic radio jets observed on 1997 October/November (Fender et al. 1999).

The radio emission during “baby jets” is consistent with synchrotron emission from an adiabatically expanding small cloud with a flat radio spectrum (Fender et al. 1997; Eikenberry et al. 1998). A magnetic field of 8–16 G and total energy $\geq 10^{40}$ erg for each half hour flare are estimated assuming equipartition. The dominant decay mechanism is adiabatic expansion losses. For a pure adiabatic expansion, the synchrotron radio luminosity $L_\nu(r) \propto r^{-2p}$, where r is the distance (eq. (19.34) of Longair (1994)). This changes to $L_\nu(r) \propto r^{-2}$ for a flat radio spectrum. For a cloud of size ~ 10 AU (minor axis at 15 GHz) and a relativistic speed of ~ 10 AU hr $^{-1}$ (Dhawan et al. 2000), a unit peak radio luminosity will decay to a value of ~ 0.44 in 15 minutes time which is in good agreement with the observations (Eikenberry et al. 1998; Mirabel et al. 1998; Pooley & Fender 1997).

The radio emission during the relativistic jets is consistent with synchrotron emission from a extended radio cloud with ballistic motion on the scale of 300–5000 AU and steepening of the spectrum with time (α changes from 0.5 to 1.0 in a few days). Atoyan & Aharonian (1999) have shown

that a single population of relativistic particles accelerated at the time of ejection cannot explain the radio emission from the relativistic jets and it requires continuous replenishment of energetic particles with energy dependent losses. Recently, Kaiser et al. (2000) have developed an internal shock model for the origin of relativistic radio jets in microquasars assuming quasi-continuous jet ejection. In this model, much of the energy needed to produce the radio emission is stored in the material of the continuous jet which was ejected by the central source prior to the formation of the shock fronts. The shock is caused by the collision of shells of jet material moving at different velocities. The formation of the internal shock ‘lights up’ the relativistic jets by accelerating particles which emit the observed synchrotron radiation. The relativistic jet mode in which strong internal shocks are produced, is thought to have strong variations in the jet speed. This is consistent with the observed X-ray color $HR_1 \geq 1.1$ in the initial phase of both the relativistic radio jets (Figure 5), which drops to a value of 0.94 in less than a day’s time (Figure 4). On the other hand, “baby jets” are supposed to represent a relatively stable mode where weak internal shocks (if any) do not play any significant role in the synchrotron emission. This is in agreement with observed values of X-ray color HR_1 which remains in the range of 0.9–1.0 for both the data sets of 1997 August 14 and September 9 (Figure 3).

4. CONCLUSIONS

We present evidence of a direct accretion disk – jet connection for relativistic radio jets. We have provided here an explanation for the most complex light curves with a “spike” observed to date in the Galactic microquasar GRS 1915+105. We suggest that the “spike” which separates the dips with hard and soft spectra marks the beginning of the burst phase, when the luminosity of the soft X-rays increases by a large factor (~ 10). This produces a major ejection episode of the synchrotron - emitting plasma termed as “baby jets” with the half-hour spacing widely reported in the literature. Subsequent short but frequent soft dips produce overlapping faint flares which result in an enhanced level of quasi-steady emission. The radio emission during “baby jets” is consistent with synchrotron emission from an adiabatically expanding small cloud (within a distance of

few tens of AU of the inner accretion disk) with a flat radio spectrum and a decay time of several minutes. On the other hand, the radio emission during the relativistic radio jets is consistent with synchrotron emission from the extended radio cloud with ballistic motion on a scale of a few hundreds to few thousands AU and a decay time of a few days. These jets require continuous replenishment of energetic particles. Our results support the relativistic jet model with quasi-continuous mass ejection and strong variations in the jet speeds required for the formation of strong internal shocks to continuously accelerate the par-

ticles.

Author thanks the referee for his very useful comments which has greatly improved the contents and the presentation of the paper. He thanks A. R. Rao and K. P. Singh for their valuable comments on the manuscript. He also thanks RXTE and NSF-NRAO-NASA Green Bank Interferometer teams for making their data publicly available. The Green Bank Interferometer is a facility of the National Science Foundation operated by the NRAO in support of NASA High Energy Astrophysics programs.

REFERENCES

Atoyan, A. M., & Aharonian, F. A. 1999, MNRAS, 302, 253
 Belloni, T., et al. 1997a, ApJ, 479, L145
 Belloni, T., et al. 1997b, ApJ, 488, L109
 Belloni, T., et al. 2000, A&A, 355, 271
 Castro-Tirado, A. J., et al. 1994, ApJS, 92, 469
 Dhawan, V., Mirabel, I. F., & Rodriguez, L. F. 2000, ApJ, in press, astro-ph/0006086
 Eikenberry S. S., et al. 1998, ApJ, 494, L61
 Eikenberry S. S., et al. 2000, ApJ, 532, L33
 Fender, R. P., et al. 1997, MNRAS, 290, L65
 Fender, R. P., & Pooley, G. G. 1998, MNRAS, 300, L65
 Fender, R. P., et al. 1999, MNRAS, 304, 865
 Feroci, M., Matt, G., Pooley, G. et al. 1999, A&A, 351, 985
 Harmon, B. A., et al. 1997, ApJ, 477, L85
 Jahoda, K. et al. 1996, SPOE 2808, 59
 Kaiser, C. R., Sunyaev, R., & Spruit, H. C. 2000, A&A, 356, 975
 Longair M. S. 1994, High Energy Astrophysics, volume 2, 2nd edition, Cambridge University Press
 Mirabel, I. F., & Rodriguez, L. F. 1994, Nature, 371, 46
 Mirabel, I. F., et al. 1998, A & A, 330, L9
 Munoz, M. P., Morgan, E. H., & Remillard, R. A. 1999, ApJ, 527, 321
 Morgan, E. H., Remillard, R. A., & Greiner, J. 1997, ApJ, 482, 993
 Naik, S. et al. 2000, Submitted to ApJ.
 Narayan, R., Barret, D., & McClintock, J.E. 1997, ApJ, 482, 448
 Orosz, J. A., & Bailyn, C. D. 1997, ApJ, 477, 876
 Pooley, G. G., & Fender, R. P. 1997, MNRAS, 292, 925
 Shrader, C., & Titarchuk, L. 1998, ApJ, 499, L31
 Tingay, S. et al. 1995, Nature 374, 141
 Yadav, J. S. et al. 1999, ApJ, 517, 935
 Yadav, J. S., 2000, under preparation.
 Yadav, J. S. & Rao A. R. 2000, ApJ (submitted for publication)

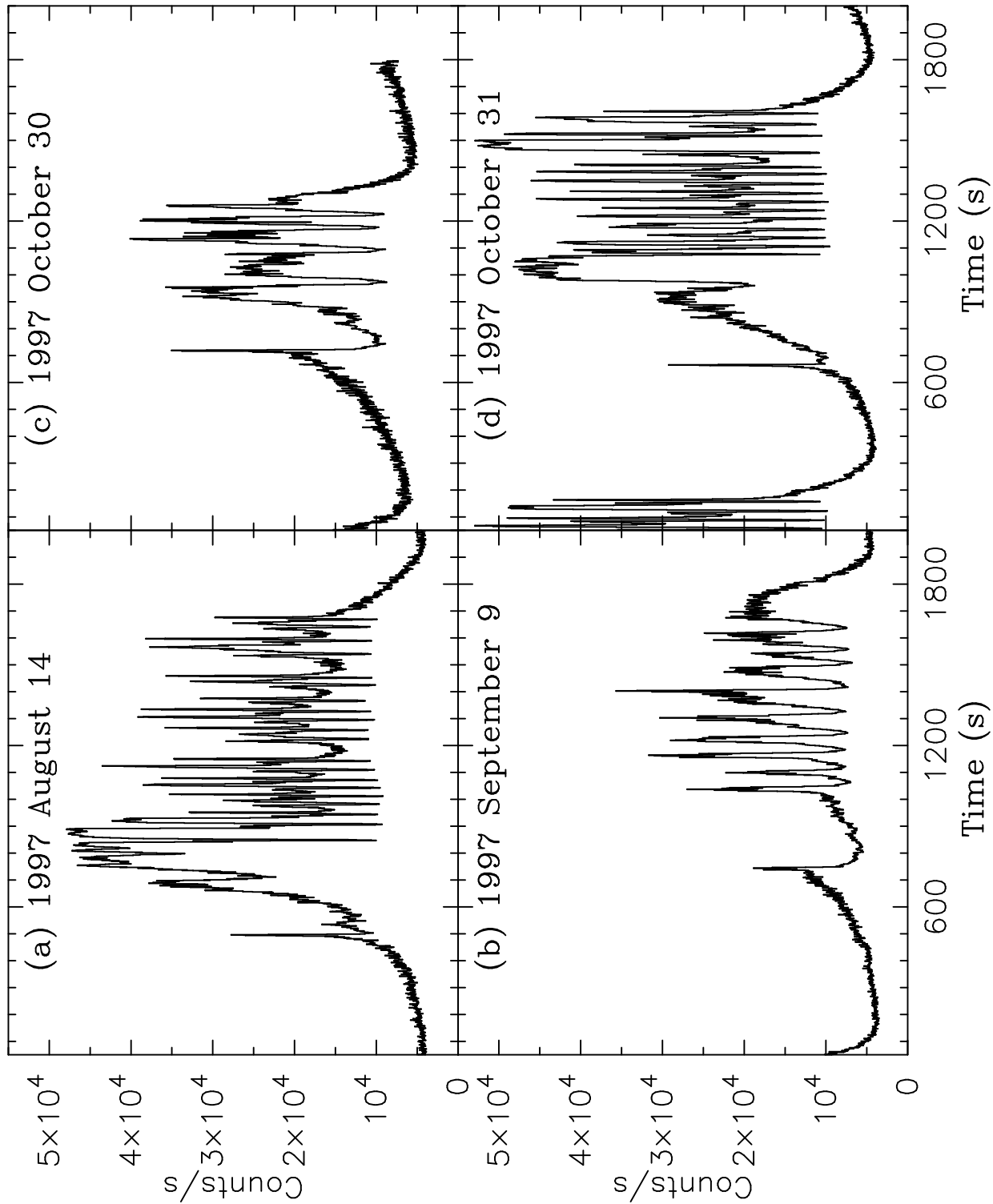


FIG. 1.— The 2–13 keV light curves of GRS 1915+105 observed on (a) 1997 August 14, (b) 1997 September 9, (c) 1997 October 30, and (d) 1997 October 31. The presence of a “spike” clearly shows that all these belong to class β . Only 4 PCUs were operating on 1997 September 9.

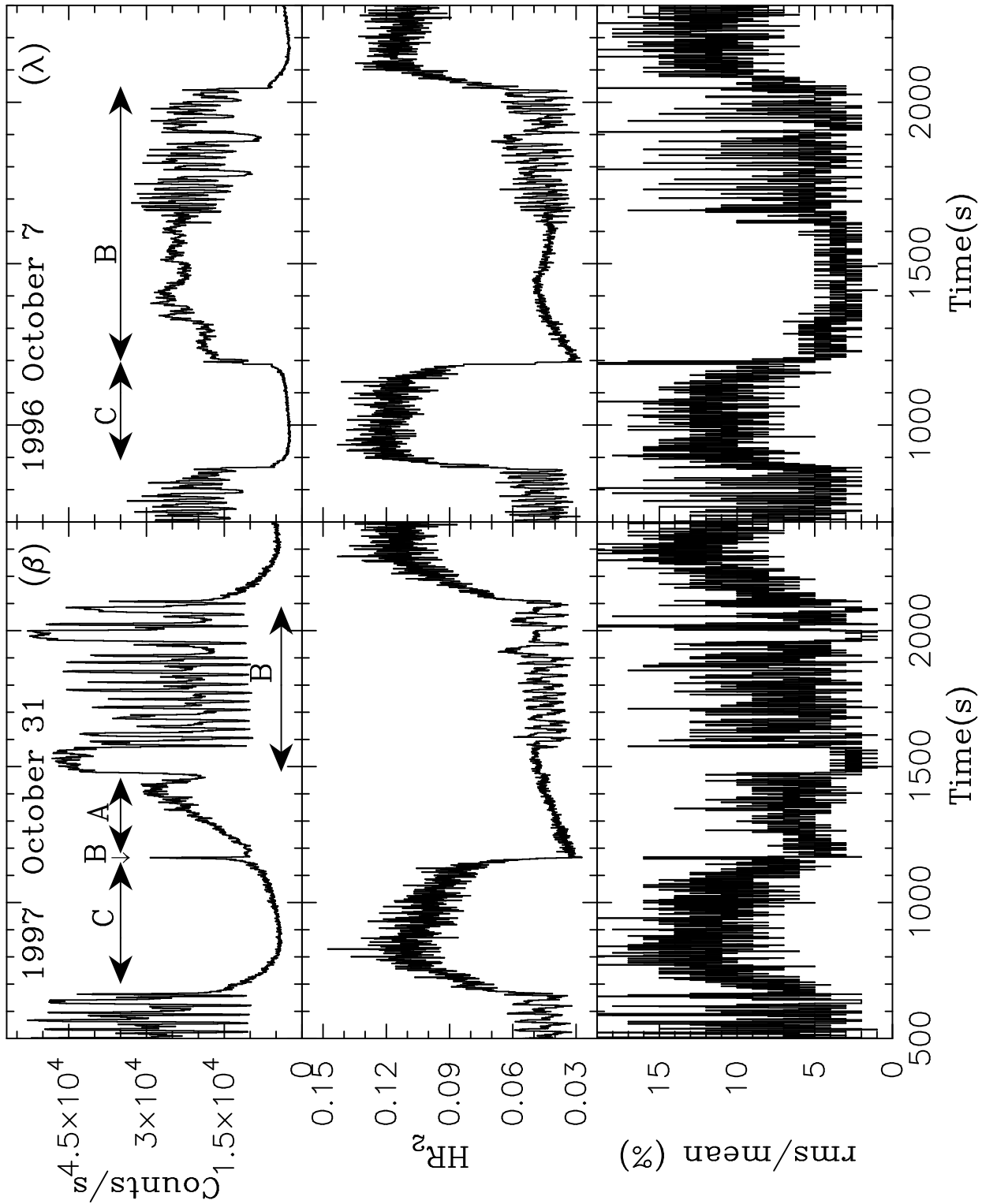


FIG. 2.— The 2–13 keV light curves of GRS 1915+105 observed on 1997 October 31 (class β) and 1996 October 7 (class λ) are shown in the top panels. The color HR_2 is shown in the middle panels and sub-second mean variability is shown in the bottom panels. In the top panels, durations of the low hard state (quiescent phase), the high soft state (burst phase) and the soft dips (low soft state) are marked by ‘C’, ‘B’ and ‘A’, respectively (for details see the text).

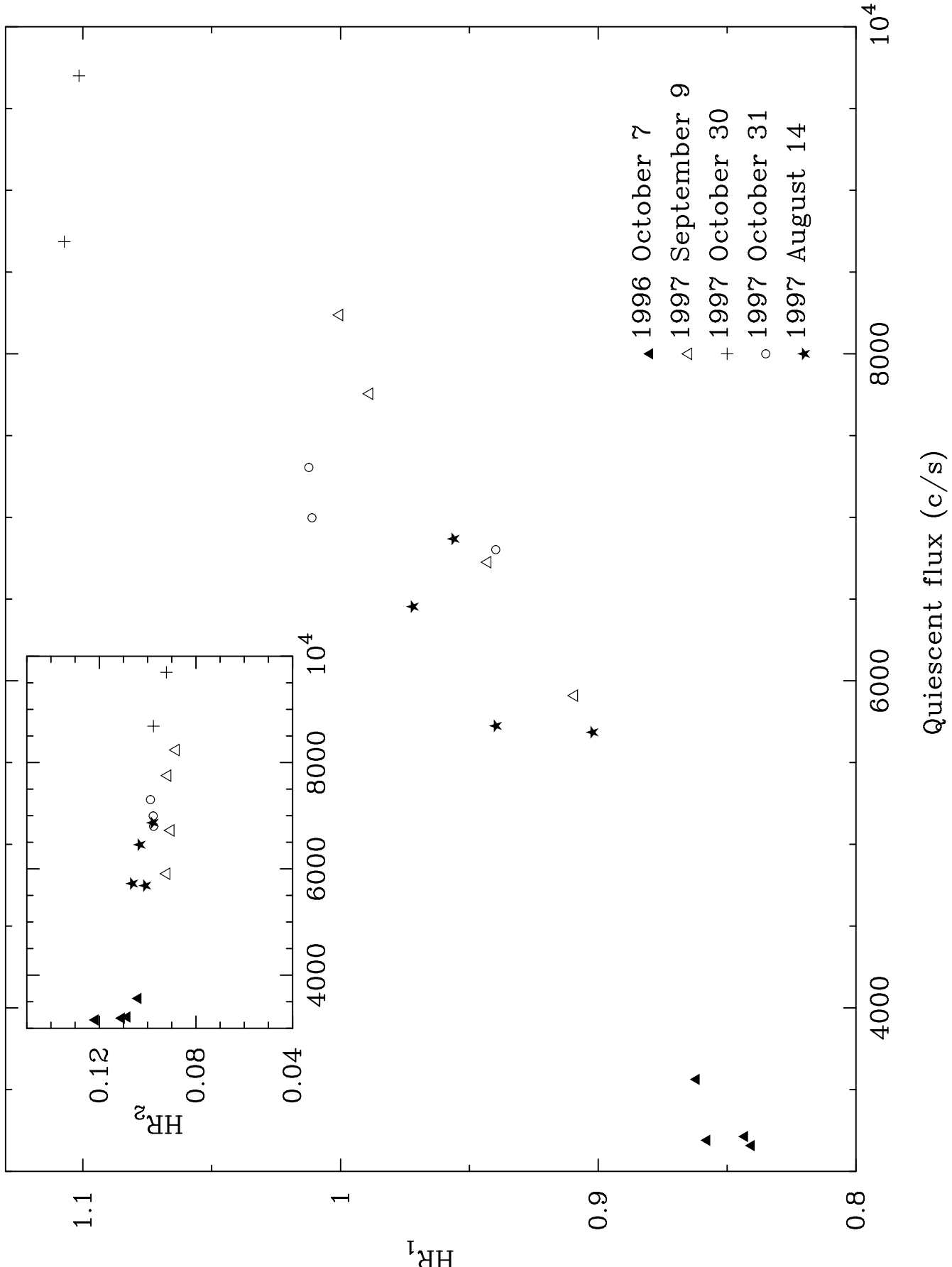


FIG. 3.— The average HR_1 during the quiescent phase (state C) is plotted as a function of average quiescent flux. The average HR_2 during the quiescent phase is shown in the inset. The HR_1 and HR_2 are defined as the ratio of the flux in the 5–13 keV band to flux in the 2–5 keV band and the ratio of the flux in the 13–60 keV band to flux in the 2–13 keV band, respectively.

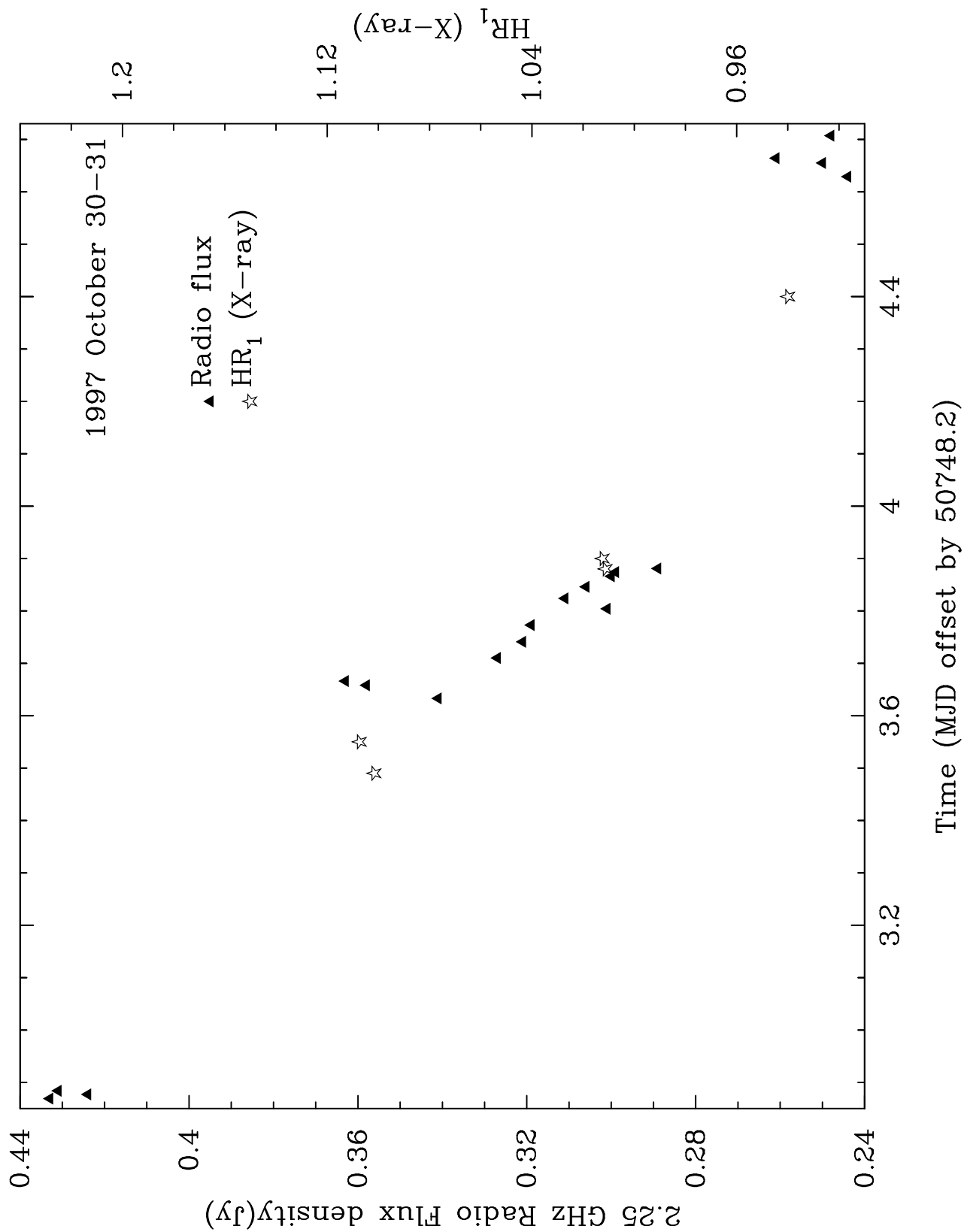


FIG. 4.— The radio flux at 2.25 GHz from the NSF-NRAO-NASA Green Bank Interferometer is plotted for 1997 October 30-31 (data for ~ 48 hours) on the y-axis (left). The X-ray average color HR_1 during the quiescent phase (state C) is plotted on the y-axis (right) during the same time (data for ~ 24 hours). Timing of X-ray observations falls between first and second relativistic radio jets observed by Fender et al. (1999).

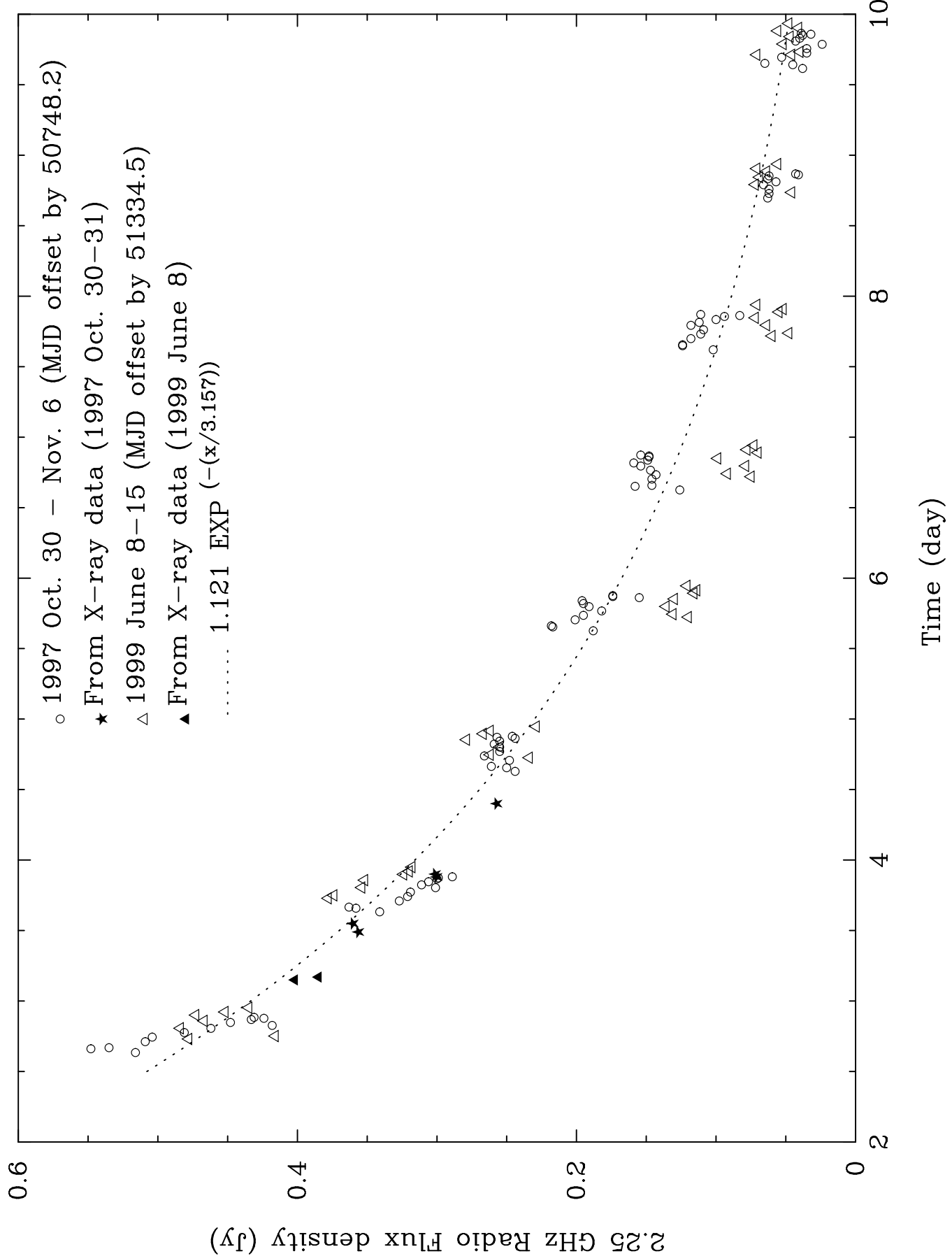


FIG. 5.— Decay profiles of two relativistic radio flares (class A) observed on 1997 October 30 - November 6 and on 1999 June 8-15. The dotted line is an exponential fit. The solid points are from X-ray data of both the flares using the relation $\text{radio}_{Jy} = 0.615 \times HR_1 - 0.322$ derived from the data of Figure 4 (for details see text).